mTOR regulates tau phosphorylation and degradation: implications for Alzheimer's disease and other tauopathies

Antonella Caccamo,1 Andrea Magrì,1* David X. Medina,1 Elena V. Wisely,1 Manuel F. López-Aranda,2 Alcino J. Silva2 and Salvatore Oddo1

1Department of Physiology and The Barshop Institute for Longevity and Aging Studies, University of Texas Health Science Center at San Antonio, 7703 Floyd Curl Drive, San Antonio, TX, 78229, USA. 2Departments of Neurobiology, Psychiatry and Biobehavioral Sciences, Psychology and the Brain Research Institute, University of California, Los Angeles, 695 Charles E. Young Dr South, Los Angeles, CA, 90095, USA

Summary

Accumulation of tau is a critical event in several neurodegenerative disorders, collectively known as tauopathies, which include Alzheimer's disease and frontotemporal dementia. Pathological tau is hyperphosphorylated and aggregates to form neurofibrillary tangles. The molecular mechanisms leading to tau accumulation remain unclear and more needs to be done to elucidate them. Age is a major risk factor for all tauopathies, suggesting that molecular changes contributing to the aging process may facilitate tau accumulation and represent common mechanisms across different tauopathies. Here, we use multiple animal models and complementary genetic and pharmacological approaches to show that the mammalian target of rapamycin (mTOR) regulates tau phosphorylation and degradation. Specifically, we show that genetically increasing mTOR activity elevates endogenous mouse tau levels and phosphorylation. Complementary to it, we further demonstrate that pharmacologically reducing mTOR signaling with rapamycin ameliorates tau pathology and the associated behavioral deficits in a mouse model overexpressing mutant human tau. Mechanistically, we provide compelling evidence that the association between mTOR and tau is linked to GSK3b and autophagy function. In summary, we show that increasing mTOR signaling facilitates tau pathology, while reducing mTOR signaling ameliorates tau pathology. Given the overwhelming evidence that reducing mTOR signaling increases lifespan and healthspan, the data presented here have profound clinical implications for aging and tauopathies and provide the molecular basis for how aging may contribute to tau pathology. Additionally, these results provide preclinical data indicating that reducing mTOR signaling may be a valid therapeutic approach for tauopathies.

Key words: AD; aging; Alzheimer's disease; autophagy; FTD; FTLD; NFT; rapamycin; tauopathies.

Introduction

Tau is a microtubule-binding protein whose function is to promote microtubule assembly and stabilization. Pathological tau protein, by contrast, exhibits altered solubility properties, forms filamentous structures and is abnormally phosphorylated at

certain residues; eventually, hyperphosphorylated tau accumulates to form neurofibrillary tangles [NFTs; (Ballatore et al., 2007)]. NFTs are hallmark lesions of several neurodegenerative disorders such as Alzheimer's disease (AD), frontotemporal dementia with Parkinsonism linked to chromosome 17, Pick's disease, progressive supranuclear palsy, and corticobasal degeneration (Ballatore et al., 2007). Collectively, these disorders are known as tauopathies.

Overexpression of mutant human tau in rodents has been a common approach to generate animal models of tauopathies. Among these models, the P301S mice were generated by overexpressing human tau harboring the P301S mutation, which is associated with frontotemporal dementia with Parkinsonism linked to chromosome 17, under the control of the mouse prion promoter (Yoshiyama et al., 2007). These mice develop age-dependent accumulation of NFTs and motor dysfunction, which leads to premature death (Yoshiyama et al., 2007).

Despite the progress made, more needs to be done to better understand the molecular mechanisms underlying pathological tau accumulation. Age is a common event across human tauopathies; indeed, even in cases where there is a clear genetic component, tau accumulation occurs as people age (Bertram & Tanzi, 2012). Similar results have been obtained in transgenic mice where usually most promoters drive expression of tau during development or shortly after birth; nevertheless, tau accumulation and the associated phenotype develops as a function of age (Bertram & Tanzi, 2012). Provided this evidence, it is plausible to assume that molecular changes occurring during aging may contribute to or facilitate tau accumulation. The mammalian target of rapamycin (mTOR) is a protein kinase that controls protein homeostasis by facilitating protein translation and inhibiting autophagy (Wullschleger et al., 2006). Overwhelming evidence has shown that reducing mTOR activity increases lifespan and healthspan (Harrison et al., 2009; Selman et al., 2009). It has also been reported that mTOR signaling is altered in AD brains (Chang et al., 2002; An et al., 2003; Peel & Bredesen, 2003; Griffin et al., 2005; Pei et al., 2008). Specifically, the levels of mTOR and its downstream targets, including p70S6K, have been reported to be higher in human AD brains (reviewed by (Pei et al., 2008). We have previously shown that rapamycin, an mTOR inhibitor, ameliorates Amyloid-beta (Ab) and tau pathology in the brains of 3xTg-AD mice, a widely used animal model of Alzheimer's disease (Oddo et al., 2003; Caccamo et al., 2010b; Majumder et al., 2011). Notably, in the 3xTg-AD mice, tau pathology is highly dependent on the accumulation of Ab, another pathological hallmark of AD (Oddo et al., 2004, 2006, 2008). Thus, it remains to be established whether the rapamycin-mediated reduction in tau in these mice was due to changes in amyloid-b or due to a direct interaction between mTOR and tau. Identifying whether there is a direct interaction between mTOR and tau will not only lead to a better understanding of the role of mTOR in AD, but it will also be crucial in determining the role of mTOR in other tauopathies.

Results

The tuberous sclerosis proteins (TSC) 1 and 2 are known negative regulators of mTOR (Wullschleger et al., 2006). Indeed, genetically reducing TSC2 causes mTOR

hyperactivity in people and rodents (Onda et al., 1999; Prabowo et al., 2013). To test for a direct link between mTOR signaling and tau, we first analyzed the brains of TSC2 heterozygous mice [$TSC2^{+/-}$. (Onda et al., 1999)]. Specifically, we measured mTOR signaling in the hippocampi of 21-month-old TSC2+/- and wild-type (WT) littermates (n = 6 per genotype) by Western blot. mTOR activity is routinely determined by measuring the steady-state levels of p70S6K phosphorylated at Thr389 and 4EBP1 phosphorylated at Ser65, which are two epitopes directly phosphorylated by mTOR (Guertin & Sabatini, 2007; Das et al., 2008). Although the levels of total p70S6K were similar between TSC2+/- and WT mice, we found that the levels of p70S6K phosphorylated at Thr389 were significantly higher in the hippocampi of the $TSC2^{+/-}$ mice (Fig. 1A–C; $P < 0.001$ obtained by unpaired t-test analysis). Consistently, total 4E-BP1 levels were similar between the two groups, while the levels of 4E-BP1 phosphorylated at Ser65 were significantly higher in the brains of the $TSC2^{+/-}$ mice (Fig. 1A, D–E). These data are consistent with previous reports showing hyperactive mTOR signaling following reduction in TSC levels (Onda et al., 1999; Prabowo et al., 2013).

To determine the effect of genetically upregulating mTOR signaling on endogenous tau, we measured total tau levels using the mouse anti-tau antibody, Tau 5. We found that total tau levels were ~1.5-fold higher in the hippocampi of the $TSC2^{+/-}$ mice compared with age-matched WT littermates. Unpaired t-test analysis indicated that this difference was statistically significant ($P < 0.001$; Fig. 1A, F). Most notably, endogenous mouse tau was phosphorylated at Ser202/Thr205, as indicated by the AT8 antibody. Indeed, the levels of AT8-positive tau were significantly higher in the hippocampi of the $TSC2^{+/-}$ mice compared with WT littermates ($P < 0.001$; Fig. 1A, G). This is highly significant given that hyperphosphorylated tau at the AT8 sites is linked to several tauopathies (Ballatore et al., 2007). To begin understanding the mechanisms leading to tau phosphorylation in the $TSC2^{+/-}$ mice, we assessed whether the function of the two major tau kinases, CDK5 and GSK3b was altered. We found that the levels of CDK5 were similar between the two groups of mice (Fig. 1A, H). We then measured the steady-state levels of total and GSK3b phosphorylated at Ser9 using Western blots. GSK3b is inactive when phosphorylated at Ser9; indeed, the levels of GSK3b phosphorylated at Ser9 inversely correlate with its activity (Cohen & Goedert, 2004). We found that the levels of total GSK3b were similar between $TSC2^{+/-}$ and WT mice (Fig. 1A, I). In contrast, the levels of GSK3b phosphorylated at Ser9 were significantly lower in the hippocampi of the $TSC2^{+/-}$ mice compared with WT mice ($P < 0.01$; Fig. 1A, J) strongly suggesting that GSK3b activity is upregulated in TSC2+/- mice. This finding is consistent with previous results that have linked mTOR and GSK3b signaling (Meske et al., 2008).

Overall, the data presented so far clearly show that genetic upregulation of mTOR signaling increases tau posphorylation (via a GSK3b-mediated mechanism) and tau levels. To analyze the mechanisms underlying the increase in tau levels, we first assessed whether there is a direct transcriptional control of tau by mTOR. Toward this end, we measured tau mRNA levels using real-time PCR. We found that tau expression was similar between WT and $TSC2^{+/-}$ mice as indicated by similar threshold values (3.25 _ 0.67 and 3.48 _ 0.71 for WT and $TSC2^{+/-}$ mice, respectively). A Student's t-test showed that these values were not statistically different from each other. To determine whether

the increase in tau levels was due to changes in tau turnover, we focused on the two major cellular protein degradation systems, the proteasome and autophagy. First, we utilized the fluorogenic substrates Bz-VGR-AMC, Suc-LLVY-AMC and Z-LLE-AMC to measure trypsin-like, chymotrypsin-like, and PGPH activities of the proteasome in the hippocampi of $TSC2^{+/-}$ and WT mice. We found no statistically significant changes in these activities between $TSC2^{+/-}$ and WT (Fig. 2A–C), suggesting that proteasome activity is not altered in the hippocampi of the $TSC2^{+/-}$ mice.

We next assessed whether changes in autophagy induction could account for the increase in tau levels. Toward this end, we measured the levels of the autophagy-related proteins Atg7 and the Atg5/Atg12 complex (which are necessary for autophagy induction) and LC3, which is an indicator of autophagy induction (Mizushima et al., 1998). Toward this end, LC3-I is post-translationally modified during autophagy induction to form LC3-II, which is incorporated into the growing autophagosome membrane (Mizushima et al., 1998). We found that the levels of Atg7 and the Atg5/Atg12 complex were significantly decreased in the hippocampi of $TSC2^{+/-}$ compared with WT mice ($P < 0.001$ for both; Fig. 2D–F). Furthermore, although the levels of LC3-I were similar between WT and TSC2+/- mice (Fig. 2D, G), the LC3-II levels were significantly lower in the hippocampi of TSC2+/- mice compared with WT mice ($P < 0.001$; Fig. 2D, H). Collectively, these data strongly suggest that mTOR hyperactivity leads to an increase in tau levels by reducing autophagy induction.

Further exploring the relation between mTOR and tau, we used a pharmacological approach to modulate mTOR signaling in a transgenic mouse model overexpressing human tau harboring the P301S mutation. These mice (herein referred to as P301S) develop a robust neuropathological phenotype, as described by (Yoshiyama et al., 2007). Specifically, these mice develop age-dependent accumulation of tau inclusions starting at 4–5 months of age. As the mice age, the tau pathology becomes more severe and is accompanied by neuronal loss around 12 months of age (Yoshiyama et al., 2007).

We have previously shown that rapamycin, an mTOR inhibitor, ameliorates Ab and tau pathology in 3xTg-AD mice, a widely used animal model of Alzheimer's disease (Caccamo et al., 2010b; Majumder et al., 2011). However, it remains to be established whether the rapamycin-mediated effects on tau pathology are due to a direct link between tau and mTOR or are simply due to a decrease in Ab levels. Toward this end, we have previously shown that decreasing Ab levels in the 3xTg-AD mice directly affects tau pathology (Oddo et al., 2004, 2006, 2008), and hence, we used the P301S mice to test for a direct link between mTOR and tau. Two-month-old prepathological P301S mice and nontransgenic (NonTg) littermates were randomly assigned to one of the following groups (n = 12 mice per group): (i) P301S mice fed rapamycin diet (P301S-Rapa); (ii) P301S mice fed the control diet (P301S-CTL); (iii) NonTg mice fed rapamycin diet (NonTg-Rapa); (iv) NonTg mice fed the control diet (NonTg-CTL). Mice were maintained on the appropriate diets for 6 months. The 2-month time-point was chosen, because at this age, the P301S mice do not show any overt pathology, which allows us to determine the effect of reducing mTOR signaling on the onset and progression of tau pathology. The rapamycin diet contained microencapsulated rapamycin at a concentration of 14.8 ng mg _1. The control diet contained empty microcapsules. Importantly, these are

the same formulations that have been shown to increase lifespan and ameliorate AD-like pathology in mice (Harrison et al., 2009; Caccamo et al., 2010b; Spilman et al., 2010; Majumder et al., 2011).

Mice were weighed before starting the rapamycin treatment and monthly thereafter. Notably, all four groups of mice gained weight throughout the experiments (Fig. 3A). A mixed-model, repeatedmeasures ANOVA indicated that there was a significant interaction between age and genotype ($P < 0.001$); however, there was no significant difference between drug treatment and genotype ($P > 0.05$). In summary, we found that the NonTg mice gained weight throughout the treatment and after 6 months of treatment, both groups of NonTg mice weighed significantly more than the P301S mice (Fig. 3A). Notably, these changes were linked to the genotype and were independent of rapamycin, as indicated by a post hoc test with Bonferroni correction.

At the end of the rapamycin treatment, mice were tested in a battery of cognitive and noncognitive behavioral tasks. Mice were initially trained in the Morris water maze (MWM), a spatial learning and memory task, to find a hidden platform using extra maze cues. Escape latency data were analyzed using a mixed-model, repeated measures ANOVA, with treatment as the categorically fixed effect, days as the numeric covariate, animals as the random effect, and escape latency as the dependent variable. We found a significant effect for days ($F = 9.585$; $P < 0.0001$), indicating that the mice significantly learned the task across sessions (Fig. 3B). However, the treatment-day interaction was not significant, indicating that all four groups of mice learned at the same pace. Taken together, we found that the P301S-CTL mice did not have any learning deficits compared with NonTg-CTL mice and that rapamycin did not enhance or diminish learning performance in P301S and NonTg mice.

The novel object recognition task was used to measure cortical and hippocampal function by observing spontaneous mouse behavior to explore a novel object (Mumby et al., 2002). During training, mice were exposed to two objects, object A and object B, and were left free to explore for 5 min. As expected, mice spent the same amount of time exploring the two objects. During the probe trials, object B was replaced with a new object. We found that the NonTg-Rapa and the NonTg-CTL mice spent 71.45 _ 2.76% and 70.45 _ 3.38% of their time, respectively, exploring the new object (Fig. 3C). Similarly, the P301S-Rapa and the P301S-CTL mice spent 69.03 _ 1.97 and 69.38 _ 3.34% of their time, respectively, exploring the new object (Fig. 3C). A two-way ANOVA indicated that there were no statistical differences among the groups ($P = 0.9$).

Given the motor deficits developed by the P301S mice (Yoshiyama et al., 2007), we next used the open-field activity test to measure general motor function. Analyses by two-way ANOVA showed a significant difference among the groups in the spontaneous activity ($P < 0.001$) and gross motor function ($P = 0.026$), as assessed by the distance covered in the activity chamber and the average speed during the test, respectively (Fig. 3D, E). We then conducted a Bonferroni's post hoc analysis to identify the group(s) responsible for the changes in spontaneous activity. We found that P301S-CTL mice performed significantly worse than the other three groups of mice ($P < 0.001$ for all comparisons). No other statistically significant differences were found indicating that the P301S-Rapa mice performed as well as the two NonTg groups (Fig. 3D). We obtained

similar results when we conducted the Bonferroni's post hoc analysis on the average speed data. Specifically, we found that the P301S-CTL mice performed significantly worse than the P301SRapa (Fig. 3E; $P < 0.05$), which performed as well as the two NonTg groups. We next assessed anxiety and stress by measuring openfield thigmotaxis and the time spent in the center of the arena. As expected, mice spent more time in the periphery compared with the center of the arena; this response was independent of the genotype or drug treatment, as no statistically significant differences were found among the different groups (Fig. 3F, G). To further evaluate motor function in the P301S mice, we tested them using the rotarod, which is widely utilized to assess motor coordination. Mice were trained for 90 s (6 trials day 1 for 3 days) on a rod at a constant speed of 15 rpm. Six 90-s probe trials were conducted on day 4 on an accelerating rod (1 rpm s^{-1}). Analysis by two-way ANOVA showed a significant difference among the groups ($P < 0.001$; Fig. 3H). We thus conducted a Bonferroni's post hoc analysis to identify the group(s) responsible for the changes in rotarod performance. We found that the P301S-CTL mice performed significantly different compared with the other three groups ($P < 0.01$ for all comparisons; Fig. 3H). Together, these data show that the P301S mice have a significant motor impairment, which is rescued by chronic rapamycin treatment. Indeed, the P301S-Rapa mice performed as well as the two NonTg groups.

At the end of the behavioral tests, mice were 8-month-old; at this age, the P301S mice show robust tau accumulation and phosphorylation. To assess the effects of rapamycin on brain tau pathology, sections from P301S-Rapa and P301S-CTL mice ($n = 6$ per group) were immunostained with AT8, which recognizes tau phosphorylated at Ser202/Thr205. We found that the number of AT8-positive neurons was markedly reduced in the hippocampus, cortex, and brain stem of P301S-Rapa mice compared with the same brain regions of P301S-CTL mice ($P < 0.01$ for all three regions; Fig. 4A–I). To further analyze the effects of rapamycin on tau pathology, we measured the steady-state levels of soluble and insoluble tau by Western blot ($n = 7$ per group). We found that the total levels of tau in whole brain homogenates from soluble and insoluble fractions were significantly lower in the P301S-Rapa compared with the P301S-CTL mice ($P < 0.01$; Fig. 4J, K, O, P). We also found that rapamycin administration significantly reduced tau phosphorylation. Indeed, the steady-state levels of tau phosphorylated at Ser202/Thr205 (detected by the AT8 antibody), Thr231/235 (detected by the AT180 antibody) and at Thr181 (detected by the AT270 antibody) were significantly lower in both soluble and insoluble fractions of rapamycin-treated transgenic mice compared with mice on the control diet ($P < 0.001$ for all comparisons except for the AT270 levels in the insoluble fraction where the P value was <0.05; Fig. 4J, L, M, O, Q–S). We also measured tau levels in NonTg mice using the tau 5 antibody. Although we found a strong trend toward a decrease in total tau levels in the rapamycin-treated NonTg mice, the results did not reach statistical significance ($P = 0.08$; Fig. S1, Supporting information).

To determine whether the effects of rapamycin were mediated by mTOR, we measured mTOR signaling in the brains of P301S-Rapa and P301S-CTL mice. Although the steady-state levels of total p70S6K and 4E-BP1 were similar between treated and untreated mice, we found a significant reduction in the levels of p70S6K phosphorylated at Thr389 and 4E-BP1 phosphorylated at Ser65 in the rapamycin-treated mice compared with mice on

control diet (Fig. 5A–E). Collectively, these data clearly indicate that rapamycin reaches its intended target in the brain (i.e., mTOR) and reduces its activity. Taken together, the data presented so far indicate that pharmacological reduction in mTOR signaling reduces tau pathology in the P301S transgenic mice.

To begin understanding the mechanism underlying the rapamycin- mediated reduction in tau phosphorylation, we focused on GSK3b as the data in Fig. 1 show its involvement in the mTOR tau relation. We found that while the steady-state levels of total GSK3b were similar between treated and untreated transgenic mice, the levels of GSK3b phosphorylated at Ser9 were significantly higher in the mice treated with rapamycin (Fig. 5A, F, G). Given that Ser9 is an inhibitory phospho-site, these data indicate that rapamycin decreases the activity of GSK3b.

Considering that total tau levels were also decreased by rapamycin treatment and the involvement of protein turnover in tau pathology, we measured tau mRNA levels, as well as proteasome and autophagy function. We found that tau expression was similar between P301S-CTL and P301S-Rapa, as indicated by similar threshold values (2.08 _ 0.2 and 2.85 _ 0.2 for P301S-CTL and P301S-Rapa, respectively). A Student's t-test showed that these values were not statistically different from each other. Similarly, we found that overall proteasome activity was similar between P301S-CTL and P301S-Rapa mice, as indicated by the lack of statistically significant changes in the trypsin-like, chymotrypsinlike, and PGPH activities of the proteasome in the brains of these mice (Fig. 6A–C). In contrast, we found that the levels of the autophagy-related proteins Atg7 and the Atg5/Atg12 complex were significantly increased in the brain of the transgenic mice receiving rapamycin (Fig. 6D–F; $P < 0.01$ for both measurements). Furthermore, while the levels of LC3-I were similar between the two groups (Fig. 6D, G), the LC3-II levels were significantly increased in the brains of the P301S-Rapa mice compared to P301S-CTL mice (Fig. 6D, H; $P = 0.03$). These results are consistent with the data showing that mTOR is a negative regulator of autophagy; thus, by reducing its activity, we have observed an increase in autophagy induction.

Discussion

Tau is a microtubule-binding protein that plays a primary role in microtubule stabilization. However, growing evidence suggests that tau may have other functions in the CNS related to protein signaling and cytoskeletal organization (Morris et al., 2011). Tau accumulates in a group of neurodegenerative disorders known as tauopathies such as AD, frontotemporal lobar degeneration, Pick's disease, and corticobasal degeneration (Ballatore et al., 2007). In these disorders, tau is hyperphosphorylated and aggregates to form insoluble inclusions that lead to the development of NFTs (Ballatore et al., 2007). Notably, recent evidence indicates that tau mediates learning and memory deficits in animal models of AD (Roberson et al., 2007), suggesting that reducing tau levels may represent a valid therapeutic approach.

Aging is the greatest risk factor for several neurodegenerative disorders, including tauopathies. For example, rare mutations in three genes have been identified as causes of AD (Bertram & Tanzi, 2012). Even in these clear cut genetic cases, the penetrance of the

mutations increases as a function of age. Similar observations have been reported for other tauopathies (Ballatore et al., 2007). However, little is known as to how aging contributes to tau accumulation. Identifying age-dependent changes in signaling pathways that could facilitate protein accumulation in the brain may offer new molecular targets for the development of new therapeutic interventions.

Overwhelming evidence from lower organisms and mammals links mTOR to aging. For example, studies from independent laboratories have shown that pharmacologically or genetically reducing mTOR signaling increases lifespan and healthspan in mice (Harrison et al., 2009; Selman et al., 2009). mTOR is a conserved protein kinase that plays a key role in controlling a balance between protein synthesis and degradation; indeed, mTOR dysregulation has been linked to several proteinopathies, such as Huntington's disease, AD and frontotemporal lobar degeneration (Sarkar & Rubinsztein, 2008; Oddo, 2012; Wang et al., 2012). Along these lines, we previously showed that pharmacologically reducing mTOR signaling with rapamycin ameliorates Alzheimer-like phenotype in transgenic mice and attenuates age-dependent cognitive decline in wild-type mice (Caccamo et al., 2010b; Majumder et al., 2011, 2012). Specifically, using the 3xTg-AD mice, a widely used animal model of Alzheimer's disease, we showed that reducing mTOR signaling with rapamycin was sufficient to ameliorate Ab and tau accumulation (Griffin et al., 2005; Meske et al., 2008). However, given that the tau pathology in the 3xTg-AD mice is highly dependent on the Ab pathology (Oddo et al., 2004, 2006, 2008), it remained to be established whether the decrease in tau in the rapamycin-treated 3xTg-AD mice was a secondary event due to a reduction in Ab pathology or whether there was a direct link between mTOR and tau. Here, we offer the first evidence in mammals of a direct link between mTOR signaling and tau accumulation. Notably, not only did we show that genetically increasing mTOR signaling increases tau levels and phosphorylation, but we also demonstrated that reducing mTOR signaling with rapamycin ameliorates tau pathology and rescues motor deficits in a mouse model of tauopathies. Our data are consistent with in vitro data suggesting that mTOR signaling regulates tau phosphorylation (Meske et al., 2008) and TOR activation enhances tau-induced neurodegeneration in a Drosophila model of tauopathies (Khurana et al., 2006). Given the data presented here and the primary role of mTOR in age-dependent proteinopathies, we propose that agedependent accumulation of tau in proteinopathies may be linked to an increase in mTOR signaling.

mTOR dysregulation is linked to several neurogenetic disorders characterized by abnormal synaptic plasticity (Gipson & Johnston, 2012). For example, mutations in the TSC1 and TSC2 genes cause mTOR hyperactivity (Prabowo et al., 2013) and individuals harboring those mutations develop tuberous sclerosis, an autosomal dominant disorder associated with mental retardation, autism and epilepsy (Consortium, 1993; van Slegtenhorst et al., 1997). Most notably, tau accumulation has been reported in patients with tuberous sclerosis. Consistent with these reports, here we show that reducing TSC2 in mice leads to mTOR upregulation and tau accumulation. Together, the human data and the data presented here strongly support a role of mTOR dysregulation in tau pathology and indicate that reducing mTOR signaling may be a valid therapeutic approach for tauopathies.

Experimental procedures

Mice and rapamycin administration

The tuberous sclerosis 2 heterozygous mice and tau P301S transgenic mice used in this work were described elsewhere (Onda et al., 1999; Yoshiyama et al., 2007). P301S and NonTg mice had ad libitum access to microencapsulated rapamycin or control diet during the treatment period.

Protein extractions

Mice were perfused with PBS, after which their brains were extracted and sagittally bisected. Half of the brain was frozen in dry ice and used for biochemical evaluation, while the other half was fixed in 4% paraformaldehyde and used for histological and immunohistochemical evaluation. Where specified, the hippocampi were extracted under a dissecting scope and frozen in dry ice. Whole brain extractions were performed as previously described (Caccamo et al., 2010c). For hippocampal extractions, frozen hippocampi were homogenized with a dounce homogenizer in 100 µL of T-PER solution (Fisher Scientific) supplemented with protease and phosphatase inhibitors. Tissue was then centrifuged at 20 000 g for 30 min at 4 °C. The supernatant fraction was used for Western blot analyses.

Western blots, immunohistochemistry and real-time PCR

Proteins were resolved using precast SDS/PAGE gels (Invitrogen, Carlsbad, CA, USA), as described previously (Caccamo et al., 2010a). Protein intensities were obtained as described by Caccamo et al. (2011). For immunohistochemistry, fixed brains were sectioned using a sliding vibratome; 50-lm-thick free-floating sections were stored in 0.02% sodium azide in PBS. The day of the immunostaining, sections were briefly washed with TBS (100 mM Tris pH 7.5; 150 mM NaCl) followed by a 30 min incubation in3% H_2O_2, to quench endogenous peroxidase activity. Next, the proper primary antibody was applied overnight at 4 °C. Sections were washed three times in TBS and then incubated with the respective secondary antibody for 1 h at room temperature and developed as described by Oddo et al. (2007). The real-time PCR experiments were conducted as previously described by Caccamo et al. (2012).

Behavioral experiments

Mice were handled for 5 days prior to the beginning of the behavioral tests. The Morris water maze was conducted in a circular plastic pool of 1.5 m in diameter. The pool was placed in a quiet room with several visual extramaze cues. Mice received four trainingtrials per day for five consecutive days. During each training trial, mice were placed in the water until they found a platform hidden under the surface of the water, which was made opaque using nontoxic paint. If a mouse failed to find the platform within 60 s, it was manually guided to the platform and allowed to remain there for 10 s. At the end of each trial, mice were returned to their home cage for 25 s. The experiments were

video recorded with a camera mounted on the ceiling and scored with the EthoVision XT tracking system (Noldus biological).

The open field was performed in a clear box (40 9 40 cm), and individual mice were allowed 10 min of free exploration. The test was recorded by a camera and scored with the EthoVision XT tracking system. The object recognition was conducted in the same box used for the open filed task. For this paradigm, two objects were placed in the arena and mice were allowed 5 min of free exploration, after which they were returned to their home cage for 10 min. Subsequently, mice were returned to the arena; this time one of the previous objects was replaced with a new one. Data were analyzed with the EthoVision XT tracking system.

The rotarod test was conducted as described by Caccamo et al. (2012). Briefly, mice received 6 trials day^{-1} for 3 days. During this learning phase, the rod was accelerated from 0 to 15 rpm in 20 s and then maintained at 15 rpm for 70 s. Probe trials were conducted 24 h after training and consisted of six sequential trials on an accelerating rod (1 rpm s^{-1}).

Proteasomal activity

Proteasomal activity was measured as we described previously (Medina et al., 2011). Briefly, 10 lL of protein extracts were incubated with 75 lM proteasomal substrates Suc-LLVY-AMC, Bz-VGR-AMC and Z-LLE-AMC (Enzo Life Sciences, Plymouth Meeting, PA, USA), which probe for chymotrypsin-like, trypsin-, and peptidylglutamyl-peptide hydrolyzing-like (PGPH) activities, respectively. Reactions were carried out in assay buffer [25 mM 4-(2-hydroxyethyl)- 1-piperazineethanesulfonic acid (HEPES), pH 7.5, 0.5 mM ethylenediaminetetraacetic acid (EDTA), 0.05% NP-40] in a total of 200 mLin black 96-well lates. Kinetic readings were taken at 37 °C every 1.5 min for 60 min (excitation 360 nm, emission 460 nm) using the Synergy HT microplate reader (BioTek, Winooski, VT, USA). Values were then normalized to protein concentration.

Statistical analyses

Behavioral data were analyzed by two-way ANOVA followed by a Bonferroni test to determine individual differences among groups as detailed in (Caccamo et al., 2010c). Student's t-test was used when suitable. Statistical evaluations were conducted with the assistance of GraphPad Prism (La Jolla, CA).

Acknowledgments

This study was supported by grants to S.O. from the National Institute on Aging (R01 AG037637), the Glenn Foundation and the William and Ella Owens Medical Research Foundation; and by a grant to A.J.S. from the National Institute on Mental Health (R01 MH084315). The authors have no conflict of interest. The funders had no role in study design, data collection, and analysis, decision to publish, or preparation of the manuscript.

Authors contribution

A.C. performed most of the experiments on the TSC2 mice and contributed to the manuscript preparation. A.M. performed most of the rapamycin experiments. D.X.M.

measured proteasome function. E.V.W. performed some of the Western blots and edited the manuscript. M.F.A. bred and aged the TSC2 mice. A.J.S. provided intellectual contribution with the TSC2 experiments. S.O. designed the experiments, analyzed and interpreted the data and wrote the manuscript.

References

An WL, Cowburn RF, Li L, Braak H, Alafuzoff I, Iqbal K, Iqbal IG, Winblad B, Pei JJ (2003) Up-regulation of phosphorylated/activated p70 S6 kinase and its relationship to neurofibrillary pathology in Alzheimer's disease. Am. J. Pathol. 163, 591–607.

Ballatore C, Lee VM, Trojanowski JQ (2007) Tau-mediated neurodegeneration in Alzheimer's disease and related disorders. Nat. Rev. 8, 663–672. Bertram L, Tanzi RE (2012) The genetics of Alzheimer's disease. Prog. Mol. Biol. Transl. Sci. 107, 79–100.

Caccamo A, Magri A, Oddo S (2010a) Age-dependent changes in TDP-43 levels in a mouse model of Alzheimer disease are linked to Abeta oligomers accumulation. Mol. Neurodegener. 5, 51.

Caccamo A, Majumder S, Richardson A, Strong R, Oddo S (2010b) Molecular interplay between mammalian target of rapamycin (mTOR), amyloid-beta, and Tau: effects on cognitive impairments. J. Biol. Chem. 285, 13107–13120.

Caccamo A, Maldonado MA, Bokov AF, Majumder S, Oddo S (2010c) CBP gene transfer increases BDNF levels and ameliorates learning and memory deficits in a mouse model of Alzheimer's disease. Proc. Natl Acad. Sci. USA 107, 22687– 22692.

Caccamo A, Maldonado MA, Majumder S, Medina DX, Holbein W, Magri A, Oddo S (2011) Naturally secreted amyloid-beta increases mammalian target of rapamycin (mTOR) activity via a PRAS40-mediated mechanism. J. Biol. Chem. 286, 8924–8932.

Caccamo A, Majumder S, Oddo S (2012) Cognitive decline typical of frontotemporal lobar degeneration in transgenic mice expressing the 25-kDa C-terminal fragment of TDP-43. Am. J. Pathol. 180, 293–302.

Chang RC, Wong AK, Ng HK, Hugon J (2002) Phosphorylation of eukaryotic initiation factor-2alpha (eIF2alpha) is associated with neuronal degeneration in Alzheimer's disease. NeuroReport 13, 2429–2432.

Cohen P, Goedert M (2004) GSK3 inhibitors: development and therapeutic potential. Nat. Rev. Drug Discovery 3, 479–487.

Consortium ECTS (1993) Identification and characterization of the tuberous sclerosis gene on chromosome 16. Cell 75, 1305–1315.

Das F, Ghosh-Choudhury N, Mahimainathan L, Venkatesan B, Feliers D, Riley DJ, Kasinath BS, Choudhury GG (2008) Raptor-rictor axis in TGFbeta-induced protein synthesis. Cell. Signal. 20, 409–423.

Gipson TT, Johnston MV (2012) Plasticity and mTOR: towards restoration of impaired synaptic plasticity in mTOR-related neurogenetic disorders. Neural Plast. 2012, 486402.

Griffin RJ, Moloney A, Kelliher M, Johnston JA, Ravid R, Dockery P, O'Connor R, O'Neill C (2005) Activation of Akt/PKB, increased phosphorylation of Akt substrates and loss and altered distribution of Akt and PTEN are features of Alzheimer's disease pathology. J. Neurochem. 93, 105–117.

Guertin DA, Sabatini DM (2007) Defining the role of mTOR in cancer. Cancer Cell 12, 9–22.
Harrison DE, Strong R, Sharp ZD, Nelson JF, Astle CM, Flurkey K, Nadon NL, Wilkinson JE, Frenkel K, Carter CS, Pahor M, Javors MA, Fernandez E, Miller RA (2009) Rapamycin fed late in life extends lifespan in genetically heterogeneous mice. Nature 460, 392–395.
Khurana V, Lu Y, Steinhilb ML, Oldham S, Shulman JM, Feany MB (2006) TORmediated cell-cycle activation causes neurodegeneration in a Drosophila tauopathy model. Curr. Biol. 16, 230–241.
Majumder S, Richardson A, Strong R, Oddo S (2011) Inducing autophagy by rapamycin before, but not after, the formation of plaques and tangles ameliorates cognitive deficits. PLoS ONE 6, e25416.
Majumder S, Caccamo A, Medina DX, Benavides AD, Javors MA, Kraig E, Strong R, Richardson A, Oddo S (2012) Lifelong rapamycin administration ameliorates age-dependent cognitive deficits by reducing IL-1beta and enhancing NMDA signaling. Aging Cell 11, 326–335.
Medina DX, Caccamo A, Oddo S (2011) Methylene blue reduces abeta levels and rescues early cognitive deficit by increasing proteasome activity. Brain Pathol. 21, 140–149.
Meske V, Albert F, Ohm TG (2008) Coupling of mammalian target of rapamycin with phosphoinositide 3-kinase signaling pathway regulates protein phosphatase 2A- and glycogen synthase kinase-3 -dependent phosphorylation of Tau. J. Biol. Chem. 283, 100–109.
Mizushima N, Noda T, Yoshimori T, Tanaka Y, Ishii T, George MD, Klionsky DJ, Ohsumi M, Ohsumi Y (1998) A protein conjugation system essential for autophagy. Nature 395, 395–398.
Morris M, Maeda S, Vossel K, Mucke L (2011) The many faces of tau. Neuron 70, 410–426.
Mumby DG, Gaskin S, Glenn MJ, Schramek TE, Lehmann H (2002) Hippocampal damage and exploratory preferences in rats: memory for objects, places, and contexts. Learn. Mem. 9, 49–57.
Oddo S (2012) The role of mTOR signaling in Alzheimer disease. Front. Biosci. (Schol. Ed.) 4, 941–952.
Oddo S, Caccamo A, Shepherd JD, Murphy MP, Golde TE, Kayed R, Metherate R, Mattson MP, Akbari Y, LaFerla FM (2003) Triple-transgenic model of Alzheimer's disease with plaques and tangles: intracellular Abeta and synaptic dysfunction. Neuron 39, 409–421.
Oddo S, Billings L, Kesslak JP, Cribbs DH, LaFerla FM (2004) Abeta immunotherapy leads to clearance of early, but not late, hyperphosphorylated tau aggregates via the proteasome. Neuron 43, 321–332.
Oddo S, Vasilevko V, Caccamo A, Kitazawa M, Cribbs DH, LaFerla FM (2006) Reduction of soluble Abeta and tau, but not soluble Abeta alone, ameliorates cognitive decline in transgenic mice with plaques and tangles. J. Biol. Chem. 281, 39413–39423.

Oddo S, Caccamo A, Cheng D, Jouleh B, Torp R, LaFerla FM (2007) Genetically augmenting tau levels does not modulate the onset or progression of Abeta pathology in transgenic mice. J. Neurochem. 102, 1053–1063.
Oddo S, Caccamo A, Tseng B, Cheng D, Vasilevko V, Cribbs DH, LaFerla FM (2008) Blocking Abeta42 accumulation delays the onset and progression of tau pathology via the C terminus of heat shock protein70-interacting protein: a mechanistic link between Abeta and tau pathology. J. Neurosci. 28, 12163–12175.
Onda H, Lueck A, Marks PW, Warren HB, Kwiatkowski DJ (1999) Tsc2(+/-) mice develop tumors in multiple sites that express gelsolin and are influenced by genetic background. J. Clin. Investig. 104, 687–695.
Peel AL, Bredesen DE (2003) Activation of the cell stress kinase PKR in Alzheimer's disease and human amyloid precursor protein transgenic mice. Neurobiol. Dis. 14, 52–62.
Pei JJ, Bjorkdahl C, Zhang H, Zhou X, Winblad B (2008) p70 S6 kinase and tau in Alzheimer's disease. J. Alzheimers Dis. 14, 385–392.
Prabowo AS, Anink JJ, Lammens M, Nellist M, van den Ouweland AM, Adle- Biassette H, Sarnat HB, Flores-Sarnat L, Crino PB, Aronica E (2013) Fetal Brain Lesions in Tuberous Sclerosis Complex: TORC1 Activation and Inflammation. Brain Pathol. 1, 45–59.
Roberson ED, Scearce-Levie K, Palop JJ, Yan F, Cheng IH, Wu T, Gerstein H, Yu GQ, Mucke L (2007) Reducing endogenous tau ameliorates amyloid beta-induced deficits in an Alzheimer's disease mouse model. Science 316, 750–754.
Sarkar S, Rubinsztein DC (2008) Huntington's disease: degradation of mutant huntingtin by autophagy. FEBS J. 275, 4263–4270.
Selman C, Tullet JM, Wieser D, Irvine E, Lingard SJ, Choudhury AI, Claret M, Al-Qassab H, Carmignac D, Ramadani F, Woods A, Robinson IC, Schuster E, Batterham RL, Kozma SC, Thomas G, Carling D, Okkenhaug K, Thornton JM, Partridge L, Gems D, Withers DJ (2009) Ribosomal protein S6 kinase 1 signaling regulates mammalian life span. Science 326, 140–144.
van Slegtenhorst M, de Hoogt R, Hermans C, Nellist M, Janssen B, Verhoef S, Lindhout D, van den Ouweland A, Halley D, Young J, Burley M, Jeremiah S, Woodward K, Nahmias J, Fox M, Ekong R, Osborne J, Wolfe J, Povey S, Snell RG, Cheadle JP, Jones AC, Tachataki M, Ravine D, Sampson JR, Reeve MP, Richardson P, Wilmer F, Munro C, Hawkins TL, Sepp T, Ali JB, Ward S, Green AJ, Yates JR, Kwiatkowska J, Henske EP, Short MP, Haines JH, Jozwiak S, Kwiatkowski DJ (1997) Identification of the tuberous sclerosis gene TSC1 on chromosome 9q34. Science 277, 805–808.
Spilman P, Podlutskaya N, Hart MJ, Debnath J, Gorostiza O, Bredesen D, Richardson A, Strong R, Galvan V (2010) Inhibition of mTOR by rapamycin
abolishes cognitive deficits and reduces amyloid-beta levels in a mouse model of Alzheimer's disease. PLoS ONE 5, e9979.
Wang IF, Guo BS, Liu YC, Wu CC, Yang CH, Tsai KJ, Shen CK (2012) Autophagy activators rescue and alleviate pathogenesis of a mouse model with proteinopathies of the TAR DNA-binding protein 43. Proc. Natl Acad. Sci. USA 109, 15024–15029.

Wullschleger S, Loewith R, Hall MN (2006) TOR signaling in growth and metabolism. Cell 124, 471–484.
Yoshiyama Y, Higuchi M, Zhang B, Huang SM, Iwata N, Saido TC, Maeda J, Suhara T, Trojanowski JQ, Lee VM (2007) Synapse loss and microglial activation precede tangles in a P301S tauopathy mouse model. Neuron 53, 337–351.

Figures

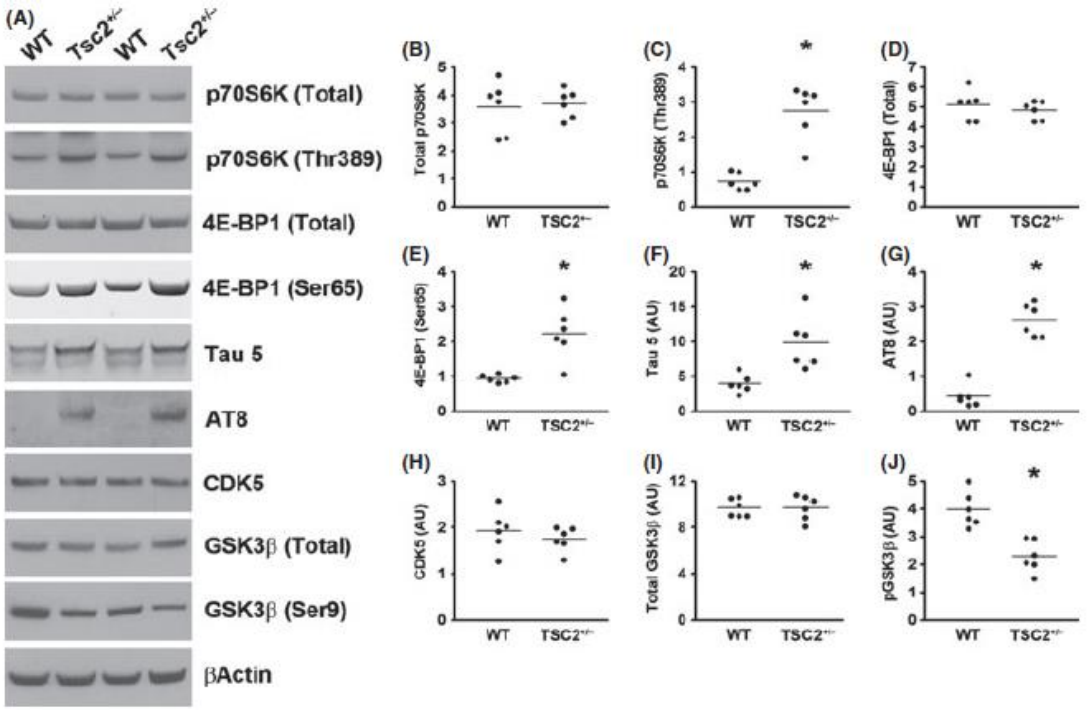

Fig. 1 mTOR signaling inversely correlates with Tau levels and phosphorylation in $TSC2^{+/-}$ mice. (A) Western blots of proteins extracted from the hippocampi of $TSC2^{+/-}$ mice and WT littermates, and probed with the indicated antibodies. (B, C) Quantitative analyses of total and phosphorylated p70S6K, respectively. Statistical analyses show that the levels of p70S6K phosphorylated at Thr389 were significantly higher in the hippocampi of the $TSC2^{+/-}$ mice compared with WT littermates. (D, E) Quantitative analyses of total and phosphorylated 4E-BP1, respectively, showed that the levels of 4E-BP1 phosphorylated at Ser65 were significantly higher in the hippocampi of the $TSC2^{+/-}$ mice compared with WT littermates. (F, G) Quantitative analyses of total (detected by the tau 5 antibody) and phosphorylated (detected by the AT8 antibody) tau showed that endogenous mouse levels were significantly higher in the hippocampi of the $TSC2^{+/-}$ mice compared with WT littermates. (H) Quantitative analyses of the CDK5 band showed no differences between the two groups of mice. (I, J) Quantitative analyses of the total and phospho-GSK3b bands, respectively. Statistical analyses indicated no changes in total

GSK3b levels between the two groups. In contrast, the levels of GSK3b phosphorylated at Ser9 were significantly lower in the hippocampi of the $TSC2^{+/-}$ mice. Quantifications of the Western blots were performed by normalizing the protein of interest to b-actin, which was used as a loading control. Data are presented as means ± SEM and analyzed by Student's t-test.

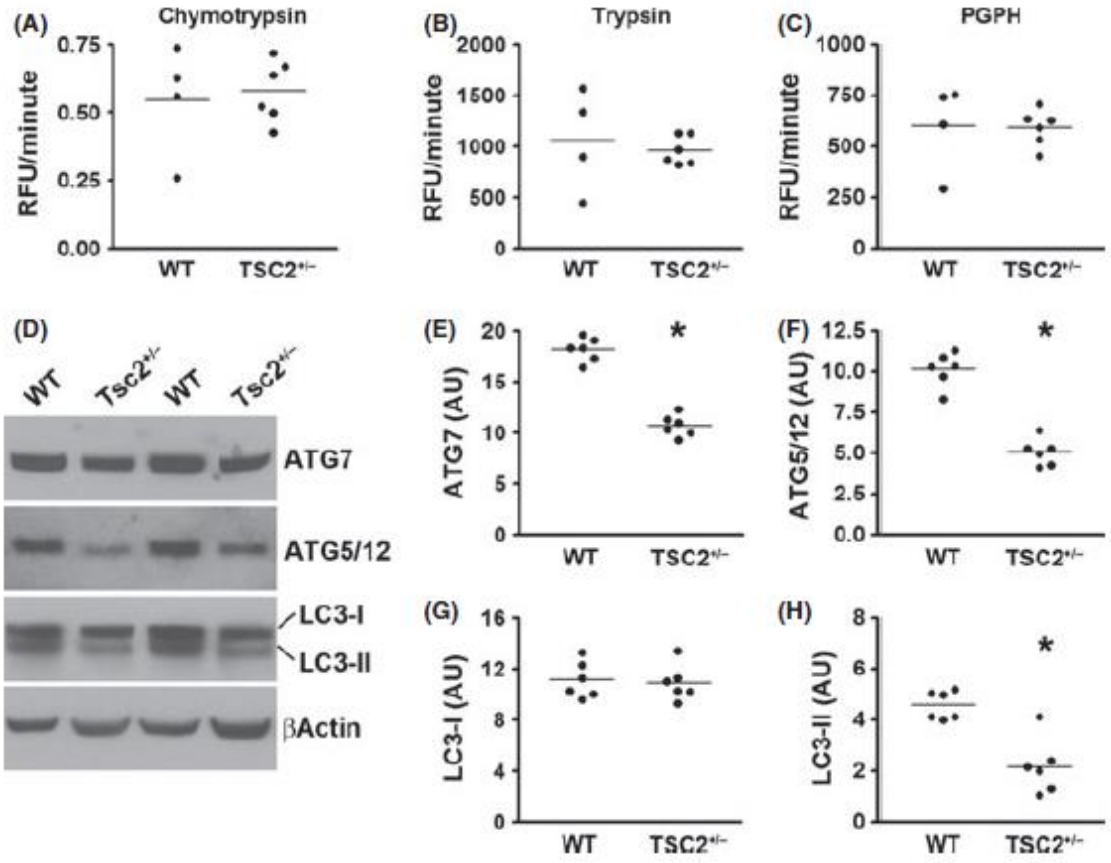

Fig. 2 Autophagy induction is decreased in the brains of $TSC2^{+/-}$ mice. (A–C) Hippocampi homogenates from $TSC2^{+/-}$ and WT littermates were analyzed for proteasome activity. The data show that removing one TSC2 allele did not alter the chymotrypsin- and trypsin-like activities, nor did it change the peptidylglutamyl-peptide hydrolyzing (PDPH) activity. (D) Western blots of proteins extracted from the hippocampi of $TSC2^{+/-}$ mice and WT littermates. (E–H) Quantitative analyses of the blots show that the levels of the autophagy-related proteins Atg7 (E) and Atg5/12 (F) were significantly decreased in $TSC2^{+/-}$ mice. Further, while quantitative analyses of the LC3-I levels showed no differences between the two groups of mice (G), LC3-II levels were significantly lower in the hippocampi of $TSC2^{+/-}$ mice compared with WT littermates (H). Quantifications of the Western blots were performed by normalizing the protein of interest to b-actin, which was used as a loading control. Data are presented as means ± SEM and analyzed by Student's t-test.

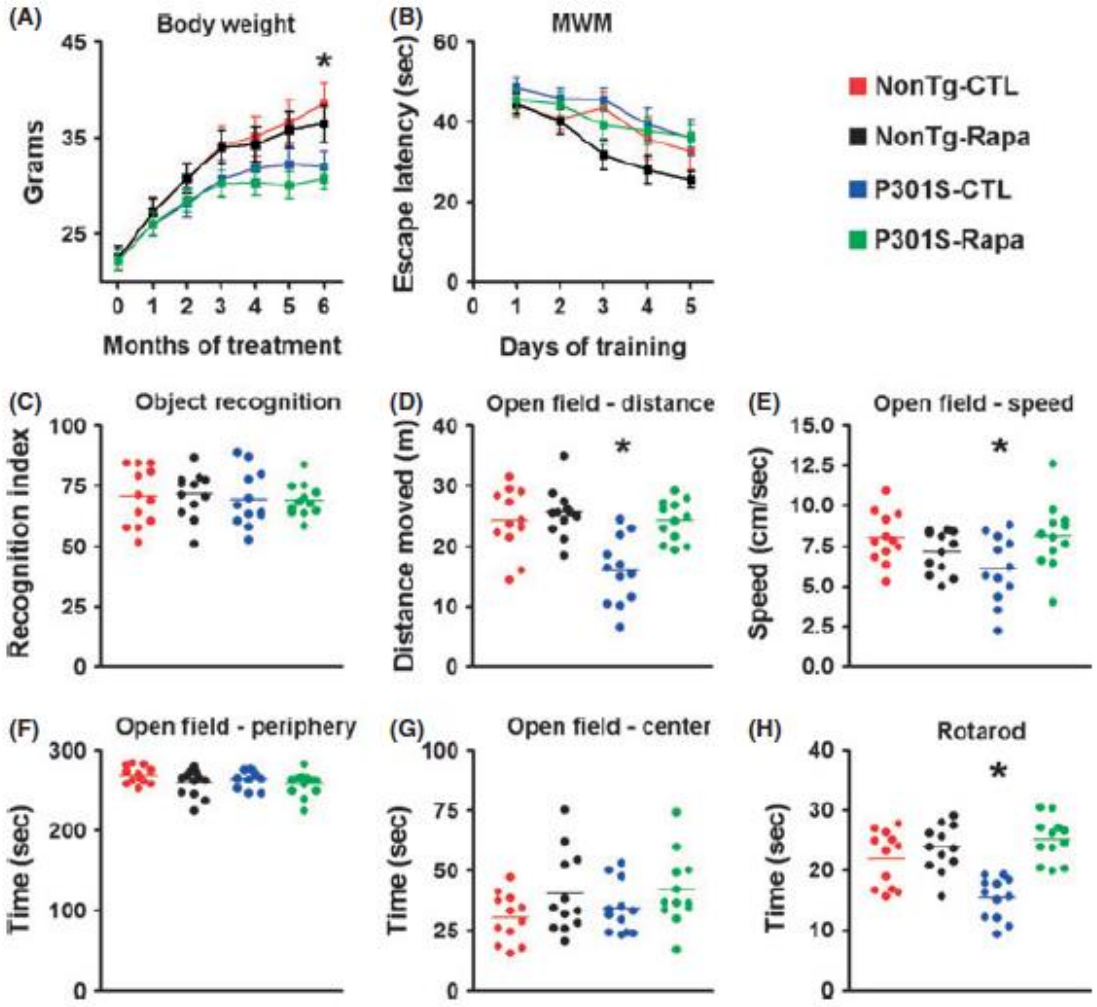

Fig. 3 Rapamycin improves motor deficits in P301S mice. (A) Transgenic P301S and NonTg mice were treated with rapamycin for 6 months. The graph shows the average body weight for each group of mice, measured monthly. Notably, the body weight of the P301S mice starts to plateau after 4 months of treatment, while the WT mice gain weight throughout the treatment period. Statistical analyses indicated that this difference was linked to the genotype and was independent of rapamycin administration. (B) Learning curve depicting mice performance in the Morris water maze. All mice significantly learned the task over the 5 days of training, as indicated by a reduced time to find the escape platform; however, no statistically significant changes were detected among the groups. (C) Novel object recognition test, a behavioral task highly dependent on the cortex, shows no differences among the four groups of mice. The graph depicts the recognition index, that is, the percentage of exploration time that mice spend exploring the new object. (D–G) Open-field activity measures spontaneous activity and anxiety. The data show that during the test, the P301S-CTL mice moved less (D) and at a slower speed (E) compared with the other three groups of mice. These changes were statistically significant. In contrast, no differences among the groups were found when measuring the

time spent in the periphery and center of the arena (F and G, respectively), indicating that the P301S mice had no detectable anxiety defects and that rapamycin did not alter this normal condition. (H) The graph shows data obtained with the accelerating rotarod. Statistical evaluation indicated that the P301S-CTL mice were significantly impaired in this task and that rapamycin administration rescued this motor deficit. Indeed, the P301S-Rapa mice performed as well as the two NonTg groups. Data are presented as means ± SEM and were analyzed by two-way ANOVA followed by a Bonferroni's test to determine individual differences among groups.

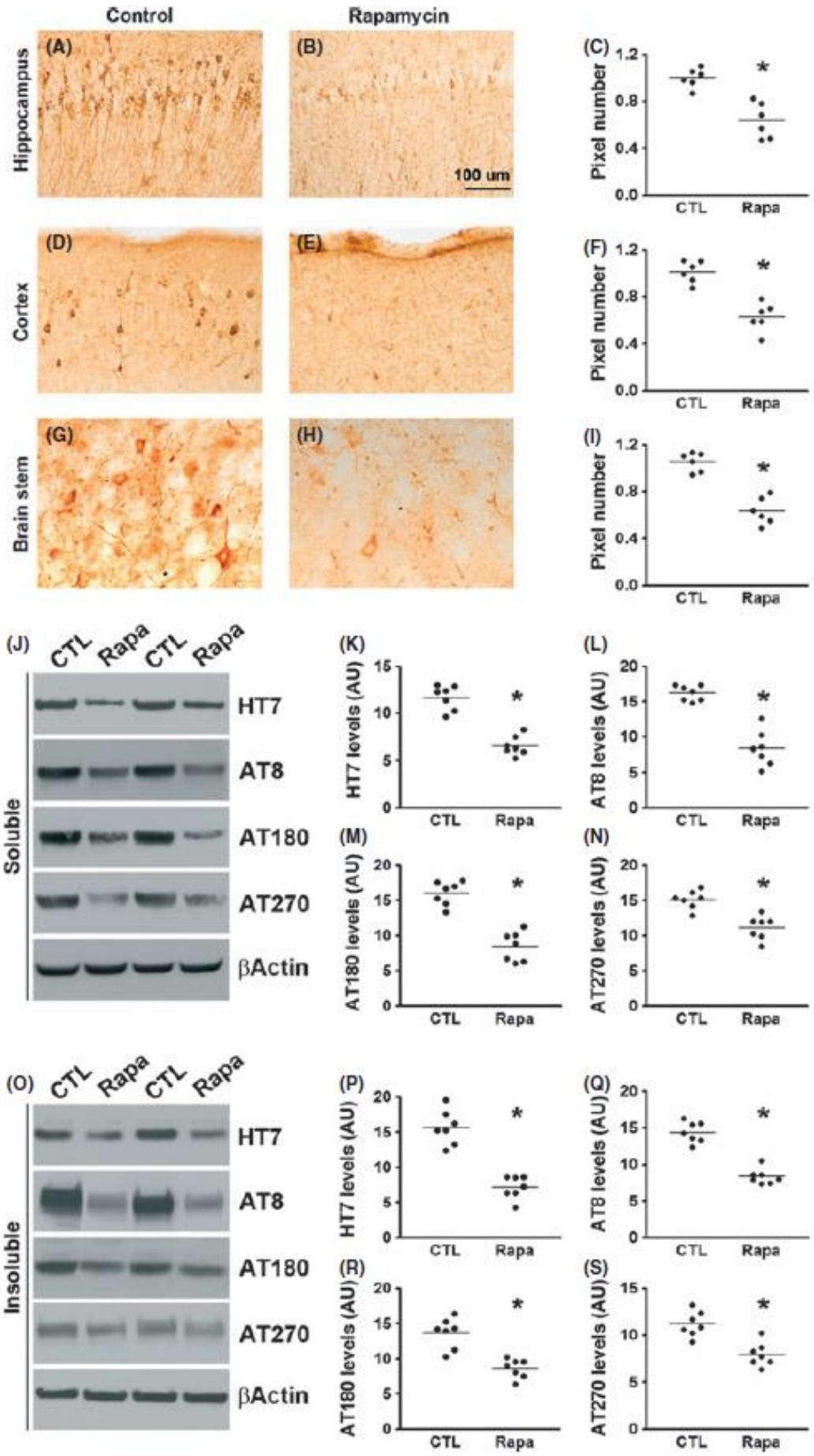
Control
Rapamycin
Hippocampus
Cortex
Brain stem
(A)
(B)
(C)
(D)
(E)
(F)
(G)
(H)
(I)
100 um
Pixel number
CTL
Rapa
(J)
CTL
Rapa
CTL
Rapa
Soluble
HT7
AT8
AT180
AT270
βActin
(K)
HT7 levels (AU)
(L)
AT8 levels (AU)
(M)
AT180 levels (AU)
(N)
AT270 levels (AU)
(O)
Insoluble
(P)
(Q)
(R)
(S)

Fig. 4 Rapamycin decreases tau pathology in P301S mice. (A–I) Microphotographs and quantitative analyses of P301S mice treated with rapamycin or control diet and stained with the AT8 antibody. (J) Western blots of soluble tau extracted from the brains of P301S mice treated with rapamycin or control diet and probed with the indicated antibodies. (K–N) Quantitative analyses of the blots show that rapamycin treatment significantly decreased the levels of tau phosphorylated at the AT8, AT180 and AT270 epitopes. (O) Western blots of insoluble tau extracted from the brains of P301S mice treated with rapamycin or control diet and probed with the indicated antibodies. (P–S) Quantitative analyses of the blots show that rapamycin significantly decreased the levels of tau phosphorylated at the AT8, AT180, and AT270 epitopes. Quantifications of the Western blots were performed by normalizing the protein of interest to b-actin, which was used as a loading control. Data are presented as means ± SEM and analyzed by Student's t-test.

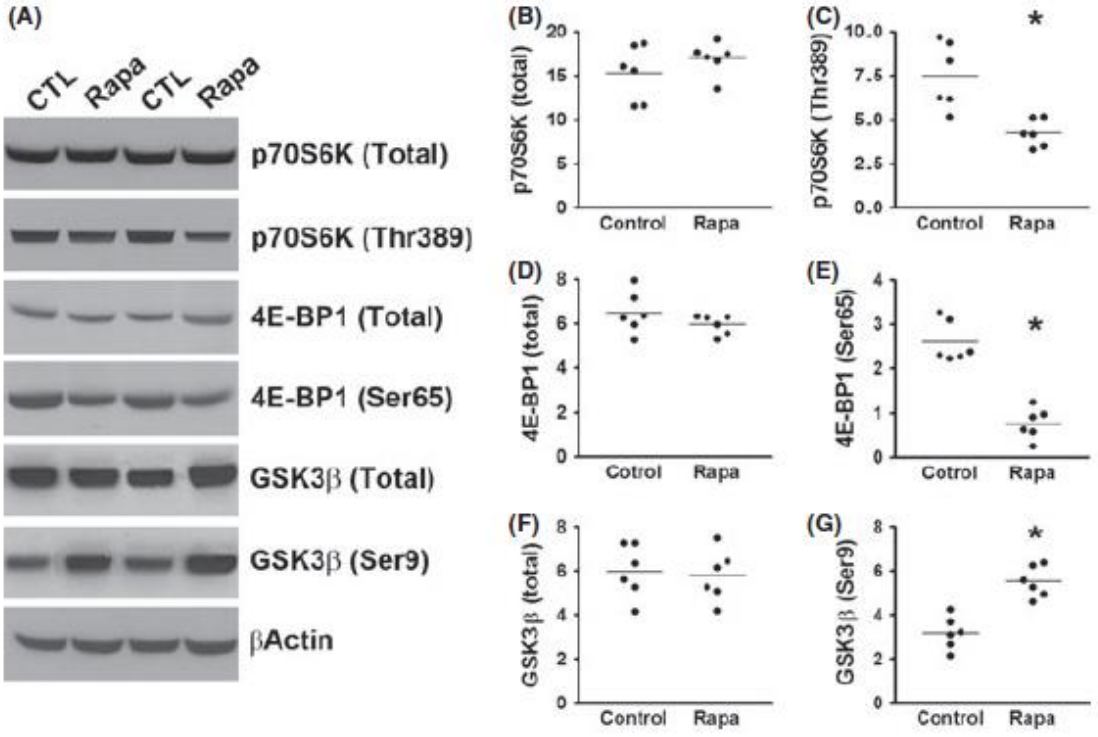

Fig. 5 mTOR signaling is decreased in P301S mice treated with rapamycin. (A) Western blots of proteins extracted from the brains of P301S mice treated with rapamycin or control diet and probed with the indicated antibodies. (B–E) Quantitative analyses of the blots show that the levels of p70S6K phosphorylated at Thr389 and 4E-BP1 phosphorylated at Ser65 were significantly lower in the rapamycin-treated mice compared with the mice on control diet. (F, G) Quantitative analyses of the blots show that the levels of GSK3b phosphorylated at Ser9 were significantly lower in the rapamycin-treated mice compared with the mice on control diet, while no difference was detected for total GSK3b levels. Quantifications of the Western blots were performed by

normalizing the protein of interest to b-actin, which was used as a loading control. Data are presented as means ± SEM and analyzed by Student’s t-test.